Journal of Fluids and Structures (2000) **14**, 1–24
doi:10.1006/jfls. 1999.0224, available online at http://www.idealibrary.com on IDEAL

LINEAR IN-PLANE AND OUT-OF-PLANE LATERAL VIBRATIONS OF A HORIZONTALLY ROTATING FLUID-TUBE CANTILEVER

D. A. PANUSSIS[1] AND A. D. DIMAROGONAS[2]

[1] *Genome Sequencing Center, Washington University School of Medicine Saint Louis, Missouri, U.S.A.*

[2] *Department of Mechanical Engineering, School of Engineering, Washington University Saint Louis, Missouri, U.S.A.*

(Received 28 July 1998 and in revised form 19 February 1999)

The case of simultaneous in-plane and out-of-plane lateral vibrations of small amplitude of a horizontally rotating fluid-tube cantilever conveying fluid is investigated. The rotation is with respect to a vertical axis at the fixed end at a constant angular velocity. The diameter of the tube is constant along its length and much smaller than the length. There is no nozzle attached at the free end. The fluid-tube cantilever is inextensible. Two inter-dependent equations of motion in the two directions of lateral displacement of the system are derived by means of Newton's second law on a fluid-tube element. The same system of equations is derived by means of Hamilton's principle. An approximate solution is sought in the case of linear vibrations in the form of a series of normalized eigenfunctions from the linear cantilever beam theory using Galerkin's method. The critical nondimensional circular frequency of lateral vibration and critical nondimensional speed of flow of the fluid-tube cantilever system are investigated for the in-plane and the out-of-plane case. Comparisons between the in-plane and out-of-plane case, between the rotating and the nonrotating case, as well as between the rotating with internal flow and the rotating case without flow are discussed. © 2000 Academic Press

1. INTRODUCTION

THE STATIONARY CANTILEVER TUBE conveying fluid and the rotating uniform cantilever beam without flow are the closest prior art to the rotating flexible fluid-tube cantilever system. The stability of the former two systems has been extensively studied independently of each other. In the current literature, no distinction has been made between rotating and nonrotating fluid-tube cantilevers, since only the latter type has been investigated until now. However, in the present work, the above terminology will be used, in order to distinguish the rotating type from the nonrotating one.

The earliest published study on the stability of nonrotating fluid-tube cantilevers was by Bourrières in 1939 (Païdoussis & Issid 1974), however without computing the critical conditions for instability of the fluid-tube cantilever system. More complete theoretical and experimental studies were done later, firstly for nonrotating articulated pipes (Benjamin 1961a, b) and then for nonrotating continuous horizontal flexible tubular cantilevers conveying fluid (Gregory & Païdoussis 1966a, b). The critical conditions for instability for out-of-plane lateral vibrations of the nonrotating fluid-tube cantilever system have been calculated using an exact and an approximate method (Gregory & Païdoussis 1966a). Research in fluid–structure interaction has seen a vast expansion, to include a variety of geometry types for the structure and fluid flow types (Chen 1987; Blevins 1990). Over the

0889–9746/00/010001+24 $35.00/0 © 2000 Academic Press

years, there have been cases of practical interest, which have lent themselves as potential areas of application for theories of fluid–structure interactions involving cylindrical structures (Païdoussis 1993). Throughout the research done so far, the fluid–structure system, seen from a coordinate system fixed in space, does not undergo any motion other than the flow of fluid and the oscillatory motion generated by some instability mechanism.

On the other hand, the model of the uniform rotating beam has been employed to study the behaviour of rotating rotor blades in a variety of applications. The model of the rotating cantilever beam has been used to study rotating structures, such as robotic manipulators, helicopter rotor blades, propeller blades, wind turbines, and turbomachinery. The dynamics of a rotating cantilever beam differ from that of the nonrotating one because of the additional centrifugal stiffness and Coriolis force terms (Houbolt & Brooks 1957). Extensive research has been done on the dynamics of helicopter rotor blades in a variety of rotor configurations and load conditions (Johnson 1994). A general theory for coupled flapwise, chordwise and torsional vibrations under arbitrary loading can be found in Houbolt & Brooks (1957), along with selected linear applications. An exact solution (Du *et al.* 1994) and an approximate formula (Peters 1973) for the natural frequencies and mode shapes for out-of-plane lateral vibrations of the rotating uniform cantilever linear Euler–Bernoulli beam have been derived.

The present work links the two aforementioned broad categories of mechanical systems to represent a system with hybrid characteristics. This is a theoretical investigation of the operating conditions which may destabilize a hypothetical rotating tubular fluid dispenser. The system assumes the form of a tubular cantilever beam rotating in a horizontal plane at a constant angular speed, while delivering a constant flow at the same time. The linear Euler–Bernoulli beam model was used, assuming displacements of small amplitude. The effect of shear deformation and rotary inertia are considered to be small when compared with the effect of bending. While preliminary data have been presented earlier (Panussis & Dimarogonas 1997), this paper contains an expanded range of dynamic stability results. Also, it compares the case of the rotating fluid-tube cantilever system with the stationary cantilever conveying fluid, as well as the rotating uniform cantilever beam without inner flow.

2. HORIZONTALLY ROTATING FLUID-TUBE CANTILEVER SYSTEM

The tubular cantilever is considered to be of constant inner diameter and section properties, inextensible, of homogeneous and isotropic material, with mass per unit length m_T. The inner diameter D is much smaller than the length L. It is assumed that the tube wall thickness is such that shell-type instabilities do not develop. The flow in the tube is considered to be incompressible, with fluid density ρ_F and constant flow velocity U. The inner flow is assumed to remain constant during vibration. That is, any small-scale flow details developed on the inner flow due to small-amplitude lateral vibrations are negligible compared with the main flow. The vector of the flow velocity is always tangent to the displaced elastic axis of the tubular cantilever and parallel to the unit vector tangent $\mathbf{e}_t$ (Figure 1). There is no nozzle attached to the free end, and there are no external forces applied to the system other than gravity and the clamping shear force and bending moment applied at the fixed end of the cantilever. The fluid-tube cantilever system is considered without interior or exterior damping.

The fixed end of the fluid-tube cantilever is on the axis of rotation. The fluid-tube cantilever rotates with respect to an orthogonal inertial coordinate system $OXYZ$ fixed in space. The vector of the constant angular velocity $\mathbf{\Omega}_0$ coincides with the Z-axis of the

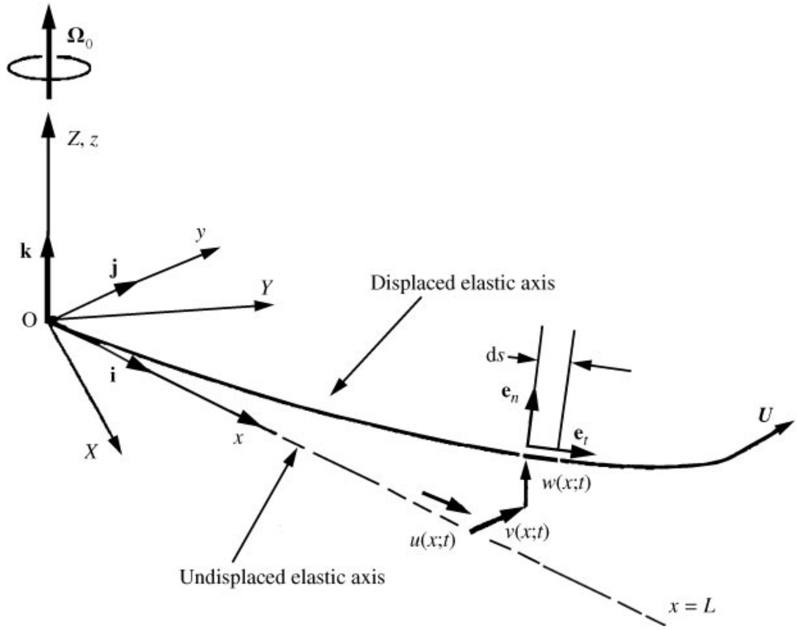

Figure 1. Schematic of the coordinate systems and the displacements of the elastic axis of the rotating fluid-tube cantilever system. The coordinate system $Oxyz$ is attached to the rotating fluid-tube cantilever, whereas $OXYZ$ is an inertial coordinate system.

inertial coordinate system. The rotation takes place on the plane OXY. A second orthogonal coordinate system $Oxyz$ rotates with respect to the inertial one at the angular velocity $\mathbf{\Omega}_0$. The x-axis coincides with the undisplaced elastic axis of the tubular cantilever. The unit vectors along the x-, y-, and z-axis are $\mathbf{i}$, $\mathbf{j}$, and $\mathbf{k}$, respectively. The position vector along the elastic axis is $\mathbf{r}_o(x; t) = x\mathbf{i}$ in the undisplaced state. The fixed end of the cantilever corresponds to $x = 0$ and the free end to $x = L$. When the rotating fluid-tube cantilever system vibrates, a fluid-tube element of finite length δx, at position x on the undisplaced elastic axis, is displaced through the axial displacement $u(x; t)$, the in-plane lateral displacement $v(x; t)$, and the out-of-plane lateral displacement $w(x; t)$, in the direction of the x-, y-, and z-axis, respectively. Hence, in the $Oxyz$ coordinate system, the position vector of the displaced element is

$$\mathbf{r}(x; t) = [x + u(x; t)]\mathbf{i} + v(x; t)\mathbf{j} + w(x; t)\mathbf{k}. \tag{1}$$

In this case, the axial displacement $u(x; t)$ is the geometrical result of the lateral displacements $v(x; t)$ and $w(x; t)$. The finite length $\delta s(x; t)$ of a fluid-tube element in the displaced state, can be expressed in terms of the finite displacements $\delta u(x; t)$, $\delta v(x; t)$ and $\delta w(x; t)$, along the x-, y- and z-axis, respectively,

$$[\delta s(x; t)]^2 = [\delta x + \delta u(x; t)]^2 + [\delta v(x; t)]^2 + [\delta w(x; t)]^2. \tag{2}$$

The requirement for inextensibility implies that the fluid-tube element maintains its length while it vibrates, i.e., at any time instant t, $\delta s(x; t) = \delta x$. When the length δx becomes small, neglecting the terms of third and higher order yields

$$\frac{\partial u(x; t)}{\partial x} \simeq -\frac{1}{2}\left[\left(\frac{\partial v(x; t)}{\partial x}\right)^2 + \left(\frac{\partial w(x; t)}{\partial x}\right)^2\right]. \tag{3}$$

Integration of equation (3) with respect to position ψ along the undisplaced elastic axis, from $\psi = 0$ at the fixed end, to $\psi = x$ at the current position x, and the geometrical condition at the fixed end that $u(0; t) = 0$ yield

$$u(x; t) = -\frac{1}{2}\int_0^x \left\{\left[\frac{\partial v(\psi; t)}{\partial \psi}\right]^2 + \left[\frac{\partial w(\psi; t)}{\partial \psi}\right]^2\right\} \mathrm{d}\psi. \tag{4}$$

The unit vector $\mathbf{e}_t(x; t) = \partial \mathbf{r}(x; t)/\partial s$ (O'Neil 1991) tangent to the displaced elastic axis at position x at time t becomes

$$\mathbf{e}_t = \frac{\partial \mathbf{r}}{\partial x}. \tag{5}$$

If $R(x; t)$ is the total curvature of the displaced elastic axis at position x at the time instant t, measured along the unit vector $\mathbf{e}_n(x; t) = (1/R(x; t))(\partial \mathbf{e}_t(x; t)/\partial s)$ (O'Neil 1991), normal to the displaced elastic axis, then

$$\mathbf{e}_n = \frac{1}{R}\frac{\partial \mathbf{e}_t}{\partial x}. \tag{6}$$

The axial coordinate x is of the same order of magnitude as the length L. The lateral displacements of in-plane and out-of-plane, $v(x; t)$ and $w(x; t)$, are of the same order of magnitude as the internal diameter D of the rotating fluid-tube cantilever, assumed to be much smaller than its length L. Equation (4) implies that the axial displacement $u(x; t)$ is one order of magnitude smaller than $v(x; t)$ and $w(x; t)$. Introducing a parameter ε, which is much smaller than unity ($\varepsilon \ll 1$), the following relations apply:

$$\mathcal{O}(v/L) = \varepsilon, \quad \mathcal{O}(w/L) = \varepsilon, \quad \mathcal{O}\left(\frac{\partial v(x; t)}{\partial x}\right) = \varepsilon, \quad \mathcal{O}\left(\frac{\partial w(x; t)}{\partial x}\right) = \varepsilon, \quad \mathcal{O}\left(\left[\frac{\partial v(x; t)}{\partial x}\right]^2\right) = \varepsilon^2,$$

$$\mathcal{O}\left(\left[\frac{\partial w(x; t)}{\partial x}\right]^2\right) = \varepsilon^2, \quad \mathcal{O}\left(\left[\frac{\partial v(x; t)}{\partial x}\right]\left[\frac{\partial w(x; t)}{\partial x}\right]\right) = \varepsilon^2, \quad \mathcal{O}\left(\frac{u(x; t)}{L}\right) = \varepsilon^2. \tag{7}$$

3. EQUATIONS OF MOTION

Two different approaches were followed for the derivation of the differential equations of motion. In the first method, Newton's second law is applied to a tube element of infinitesimal length $\mathrm{d}x$ in the undisplaced state and of mass $m_T\,\mathrm{d}x$; similarly, for the vibrating fluid element of mass $\rho_F A\,\mathrm{d}x$. From the resulting six equations, two integrodifferential equations of motion in $v(x; t)$ and $w(x; t)$ are derived. The geometric and force boundary conditions of a cantilever beam are well known (Bishop & Johnson 1960). Namely, at the fixed end, the cantilever beam is constrained to have zero displacement and zero slope. At the free end, the external bending moment and shear force are zero. The detailed procedure for the derivation of the equations using Newton's second law can be found in Panussis (1998). In the following, the methodology for the derivation of the equations of motion using the Lagrangian method is presented.

In the inertial coordinate system $OXYZ$, the velocity vector $\mathbf{v}_T = \mathbf{v}_T(x; t)$ of the deflected tube element, which was at position x on the undisplaced elastic axis, has two components. One component is the velocity of the tube element in the rotating coordinate system $Oxyz$, equal to the partial derivative with respect to time t of the position vector $\mathbf{r}(x; t)$, given in Equation (1), namely $\partial \mathbf{r}(x; t)/\partial t$. The second component is due to the rotation of the local coordinate system $Oxyz$ with respect to the inertial coordinate system $OXYZ$, namely $\mathbf{\Omega}_0 \times \mathbf{r}(x;t)$. Hence,

$$\mathbf{v}_T = \frac{\partial \mathbf{r}}{\partial t} + \mathbf{\Omega}_0 \times \mathbf{r}. \tag{8}$$

Consider the fluid element enclosed in the tube element of length dx in the undisplaced state, with mass $\rho_F A\,\mathrm{d}x$. In the rotating coordinate system $Oxyz$ in Figure 1, the material derivative $\mathrm{D}\mathbf{r}(x;t)/\mathrm{D}t$ of the position vector $\mathbf{r}(x;t)$ of the displaced fluid element in equation (1) has two components (Currie 1974). One component is due to the fact that the fluid element follows the motion of the tube element as the latter vibrates, equal to the partial derivative with respect to time t of the position vector $\mathbf{r}(x;t)$, namely $\partial\mathbf{r}(x;t)/\partial t$. The second component is due to the internal flow in the fluid-tube cantilever system, equal to $[U\mathbf{e}_t(x;t)\cdot\mathbf{\nabla}]\mathbf{r}(x;t)$. Hence,

$$\frac{\mathrm{D}\mathbf{r}}{\mathrm{D}t} = \frac{\partial \mathbf{r}}{\partial t} + U\mathbf{e}_t. \tag{9}$$

In the inertial coordinate system $OXYZ$, the velocity $\mathbf{v}_F = \mathbf{v}_F(x;t)$ of the fluid element, as in the case of the tube element, has an additional component due to the rotation $\mathbf{\Omega}_0$ of the coordinate system $Oxyz$ with respect to the inertial coordinate system $OXYZ$. That component is equal to the cross-product of the vector of the speed of rotation $\mathbf{\Omega}_0$ with the position vector $\mathbf{r}(x;t)$, namely $\mathbf{\Omega}_0 \times \mathbf{r}(x;t)$. Hence,

$$\mathbf{v}_F = \frac{\partial \mathbf{r}}{\partial t} + U\mathbf{e}_t + \mathbf{\Omega}_0 \times \mathbf{r}. \tag{10}$$

Using equation (8) for the velocity of the tube element $\mathbf{v}_T(x;t)$, the kinetic energy of the tube in the rotating fluid-tube cantilever system is

$$T_T = \frac{1}{2}\int_0^L m_T(\mathbf{v}_T \cdot \mathbf{v}_T)\,\mathrm{d}x. \tag{11}$$

With the assumption that, in this case, the shear deformation is small compared to the bending effect, the potential energy of the tube in the rotating fluid-tube cantilever system includes the flexural energy of elastic bending deformation plus the effect of gravity,

$$V_T = \frac{1}{2}\int_0^L EI\left(\frac{\partial^2 v}{\partial x^2}\right)^2 \mathrm{d}x + \frac{1}{2}\int_0^L EI\left(\frac{\partial^2 w}{\partial x^2}\right)^2 \mathrm{d}x + \int_0^L m_T g w\,\mathrm{d}x. \tag{12}$$

Using equation (10), the kinetic energy of the fluid contained at any time within the rotating fluid-tube cantilever is

$$T_F = \frac{1}{2}\int_0^L \rho_F A(\mathbf{v}_\mathrm{F} \cdot \mathbf{v}_\mathrm{F})\,\mathrm{d}x. \tag{13}$$

Consider a control volume in the flow defined by the interior of the vibrating tube portion of the fluid-tube cantilever. The control surface momentarily coincides with the fluid-tube interface and the plane end-sections of the flow, at the fixed end $x = 0$ and at the free end $x = L$. The plane end-sections of the flow are considered perpendicular to the deflected x-axis. The constant flow rate along the tube is $\rho_F AU$. During the finite time period δt, a fluid mass equal to $\rho_F AU\delta t$ enters the control volume at the fixed end $x = 0$. Given that $\mathbf{v}_F(0;t) = U\mathbf{i}$, the corresponding finite inflow of kinetic energy $\delta T_\mathrm{in}(t)$ is

$$\delta T_\mathrm{in} = \tfrac{1}{2}\rho_F AU(\mathbf{v}_F \cdot \mathbf{v}_F)_{x=0}\delta t = \tfrac{1}{2}\rho_F AU^3\,\delta t. \tag{14}$$

During the finite time period δt, a fluid mass equal to $\rho_F A U \delta t$ exits the control volume at $x = L$. The corresponding finite outflow of kinetic energy $\delta T_{\text{out}}(t)$ is

$$\delta T_{\text{out}} = \tfrac{1}{2}\rho_F A U (\mathbf{v}_F \cdot \mathbf{v}_F)_{x=L}\,\delta t, \tag{15}$$

where, $\mathbf{v}_F(x; t)$ is given by equation (10). The net finite outflow $\delta T_{\text{flux}}(t)$ of kinetic energy through the control surface during the finite period of time δt is

$$\delta T_{\text{flux}} = \delta T_{\text{out}} - \delta T_{\text{in}} = \tfrac{1}{2}\rho_F A U [(\mathbf{v}_F \cdot \mathbf{v}_F)_{x=L} - U^2]\,\delta t. \tag{16}$$

In the limit $\delta t \to \mathrm{d}t$, the flux $\dot{T}_{\text{flux}}(t)$ of kinetic energy through the control surface is

$$\dot{T}_{\text{flux}} = \frac{\mathrm{d}T_{\text{flux}}}{\mathrm{d}t} = \tfrac{1}{2}\rho_F A U [(\mathbf{v}_F \cdot \mathbf{v}_F)_{x=L} - U^2]. \tag{17}$$

The total kinetic energy of the fluid, enclosed momentarily in the control volume, equals the sum of the kinetic energy of the fluid T_F and the kinetic energy δT_{flux}, which exited from the control volume due to the flow U during the finite time period δt. Thus,

$$T_F + \dot{T}_{\text{flux}}\,\delta t = \frac{1}{2}\int_0^L \rho_F A (\mathbf{v}_F \cdot \mathbf{v}_F)\,\mathrm{d}x + \tfrac{1}{2}\rho_F A U [(\mathbf{v}_F \cdot \mathbf{v}_F)_{x=L} - U^2]\,\delta t. \tag{18}$$

The potential energy of the fluid due to gravity is

$$V_F = \int_0^L \rho_F A g w\,\mathrm{d}x. \tag{19}$$

The rotating fluid-tube cantilever system is considered to be holonomic. The position vector and the potential energy are considered to be explicit functions of N generalized coordinates $q_i(t)$ only. The velocity vector and the kinetic energy are considered to be explicit functions of the generalized coordinates $q_i(t)$ and their time derivatives $\dot{q}_i(t) = \mathrm{d}q_i(t)/\mathrm{d}t$. Following Benjamin (1961a), application of the Lagrange equations on the tube portion of the fluid-tube cantilever and on the flowing fluid mass yields the Lagrange equations for the combined fluid-tube system:

$$\frac{\mathrm{d}}{\mathrm{d}t}\left(\frac{\partial L_{FT}}{\partial \dot{q}_i}\right) - \frac{\partial L_{FT}}{\partial q_i} + \rho_F A U \left[\mathbf{v}_F \cdot \frac{\partial \mathbf{r}}{\partial q_i}\right]_{x=L} = 0, \quad i = 1, 2, \ldots, N. \tag{20}$$

In this case, $\mathbf{v}_F$ is given by equation (10) and L_{FT} is the Lagrangian function of the fluid-tube cantilever system,

$$L_{FT} = T_T + T_F - V_T - V_F. \tag{21}$$

Consider two distinct times t_1 and t_2, when the variations of the generalized coordinates are assumed to be zero, i.e.,

$$\delta[q_i(t_1)] = \delta[q_i(t_2)] = 0, \quad i = 1, 2, \ldots, N. \tag{22}$$

Equations (20) are multiplied by δq_i, added together, and integrated with respect to time t over the time interval $[t_1, t_2]$ to yield

$$\int_{t_1}^{t_2}\left[\frac{\mathrm{d}}{\mathrm{d}t}\left(\frac{\partial L_{FT}}{\partial \dot{q}_i}\right) - \frac{\partial L_{FT}}{\partial q_i}\right]\delta q_i\,\mathrm{d}t + \int_{t_1}^{t_2} \rho_F A U \left[\mathbf{v}_F \cdot \frac{\partial \mathbf{r}}{\partial q_i}\,\delta q_i\right]_{x=L}\mathrm{d}t = 0, \tag{23}$$

where, the double-index summation convention was used. Using a well-known procedure, equation (23) yields the statement of Hamilton's principle for the case of the horizontally rotating fluid-tube cantilever system:

$$\delta \int_{t_1}^{t_2} L_{FT}\, \mathrm{d}t - \int_{t_1}^{t_2} \rho_F A U [\mathbf{v}_F \cdot \delta \mathbf{r}]_{x=L}\, \mathrm{d}t = 0. \tag{24}$$

Variation of the terms in Equation (24) yields the following expression (Panussis 1998):

$$\int_{t_1}^{t_2} \int_0^L [F_v(x;t)\, \delta v + F_w(x;t)\, \delta w]\, \mathrm{d}x\, \mathrm{d}t = 0. \tag{25}$$

Since δv and δw are arbitrary, in order for equation (25) to hold, F_v and F_w must be identically equal to zero, yielding respectively the following nonlinear integrodifferential equations of motion in $v(x;t)$ and $w(x;t)$, where terms of order ε^4 and higher have been left out;

$$\begin{aligned}
&EI \frac{\partial^4 v}{\partial x^4} + (m_T + \rho_F A) \frac{\partial^2 v}{\partial t^2} + 2\rho_F A U \frac{\partial^2 v}{\partial x \partial t} + \rho_F A U^2 \frac{\partial^2 v}{\partial x^2} \\
&- (m_T + \rho_F A)\Omega_0^2 v + (m_T + \rho_F A)\Omega_0^2 x \frac{\partial v}{\partial x} \\
&+ \tfrac{1}{2}(m_T + \rho_F A)\Omega_0^2 (x^2 - L^2) \frac{\partial^2 v}{\partial x^2} \\
&+ 2\rho_F A U\, \Omega_0 + \rho_F A U\, \Omega_0 \left(\frac{\partial v}{\partial x}\right)^2 + 2\rho_F A U \Omega_0 \frac{\partial^2 v}{\partial x^2}(v - v_L) \\
&- 2(m_T + \rho_F A)\Omega_0 \frac{\partial^2 v}{\partial x^2} \left(\int_x^L \frac{\partial v}{\partial t}\, \mathrm{d}\psi \right) \\
&+ 2(m_T + \rho_F A)\Omega_0 \int_0^x \frac{\partial^2 v}{\partial \psi^2} \frac{\partial v}{\partial t}\, \mathrm{d}\psi - \rho_F A U\, \Omega_0 \left(\frac{\partial w}{\partial x}\right)^2 \\
&- 2(m_T + \rho_F A)\Omega_0 \frac{\partial w}{\partial x} \frac{\partial w}{\partial t} + 2(m_T + \rho_F A)\Omega_0 \int_0^x \frac{\partial^2 w}{\partial \psi^2} \frac{\partial w}{\partial t}\, \mathrm{d}\psi = 0,
\end{aligned} \tag{26}$$

where $v_L = v(L;t)$, and

$$\begin{aligned}
&EI \frac{\partial^4 w}{\partial x^4} + (m_T + \rho_F A)\left(\frac{\partial^2 w}{\partial t^2}\right) + 2\rho_F A U \frac{\partial^2 w}{\partial x \partial t} + \rho_F A U^2 \frac{\partial^2 w}{\partial x^2} \\
&+ (m_T + \rho_F A) g + (m_T + \rho_F A)\Omega_0^2\, \mathrm{x} \frac{\partial w}{\partial x} + \tfrac{1}{2}(m_T + \rho_F A)\Omega_0^2 (x^2 - L^2) \frac{\partial^2 w}{\partial x^2} \\
&+ 2\rho_F A U\, \Omega_0 \frac{\partial^2 w}{\partial x^2}(v - v_L) + 2\rho_F A U\, \Omega_0 \frac{\partial v}{\partial x} \frac{\partial w}{\partial x} \\
&+ 2(m_T + \rho_F A)\Omega_0 \frac{\partial v}{\partial t} \frac{\partial w}{\partial x} - 2(m_T + \rho_F A)\Omega_0 \frac{\partial^2 w}{\partial x^2} \left(\int_x^L \frac{\partial v}{\partial t}\, \mathrm{d}\psi \right) = 0.
\end{aligned} \tag{27}$$

4. NONDIMENSIONAL EQUATIONS FOR IN-PLANE AND OUT-OF-PLANE LATERAL VIBRATIONS

A set of nondimensional variables is introduced, as follows:

$$\zeta = \frac{x}{L} \quad (0 \le \zeta \le 1), \quad \tau = \left(\frac{EI}{m_T + \rho_F A}\right)^{1/2} \frac{t}{L^2} \quad (0 \le \tau < \infty), \tag{28, 29}$$

$$\xi(\zeta; \tau) = \frac{v(x; t)}{L} \quad (0 \le \xi < \infty), \quad \eta(\zeta; \tau) = \frac{w(x; t)}{L} \quad (0 \le \eta < \infty). \tag{30, 31}$$

Also, a set of nondimensional parameters is introduced as follows:
(i) nondimensional flow velocity,

$$\upsilon = \left(\frac{\rho_F A}{EI}\right)^{1/2} UL; \tag{32}$$

(ii) density ratio of the mass per unit length of the fluid $\rho_F A$ with respect to the total mass per unit length of the fluid-tube cantilever system $m_T + \rho_F A$,

$$\beta = \frac{\rho_F A}{m_T + \rho_F A} \quad (0 \le \beta \le 1); \tag{33}$$

(ii) speed ratio of the velocity $\Omega_0 L$ at the free end of the cantilever beam with respect to the speed of flow U

$$C = \frac{\Omega_0 L}{U}. \tag{34}$$

With these definitions, equations (26) and (27) yield, respectively,

$$\begin{aligned} &\frac{\partial^4 \xi}{\partial \zeta^4} + \upsilon^2 \left[1 + \frac{C^2}{2\beta}(\zeta^2 - 1)\right] \frac{\partial^2 \xi}{\partial \zeta^2} + \frac{\upsilon^2 C^2}{\beta} \zeta \frac{\partial \xi}{\partial \zeta} + 2\upsilon \beta^{1/2} \frac{\partial^2 \xi}{\partial \zeta \partial \tau} + \frac{\partial^2 \xi}{\partial \tau^2} - \frac{\upsilon^2 C^2}{\beta} \xi \\ &\quad + 2\upsilon^2 C + \upsilon^2 C \left(\frac{\partial \xi}{\partial \zeta}\right)^2 + 2\upsilon^2 C \frac{\partial^2 \xi}{\partial \zeta^2}(\xi - \xi_L) - \frac{2\upsilon C}{\beta^{1/2}} \frac{\partial^2 \xi}{\partial \zeta^2} \int_\zeta^1 \frac{\partial \xi}{\partial \tau} \mathrm{d}\phi + \frac{2\upsilon C}{\beta^{1/2}} \int_0^\zeta \frac{\partial^2 \xi}{\partial \phi^2} \frac{\partial \xi}{\partial \tau} \mathrm{d}\phi \\ &\quad - \upsilon^2 C \left(\frac{\partial \eta}{\partial \zeta}\right)^2 - \frac{2\upsilon C}{\beta^{1/2}} \frac{\partial \eta}{\partial \zeta} \frac{\partial \eta}{\partial \tau} + \frac{2\upsilon C}{\beta^{1/2}} \int_0^\zeta \frac{\partial^2 \eta}{\partial \phi^2} \frac{\partial \eta}{\partial \tau} \mathrm{d}\phi = 0 \end{aligned} \tag{35}$$

and

$$\begin{aligned} &\frac{\partial^4 \eta}{\partial \zeta^4} + \upsilon^2 \left[1 + \frac{C^2}{2\beta}(\zeta^2 - 1)\right] \frac{\partial^2 \eta}{\partial \zeta^2} + \frac{\upsilon^2 C^2}{\beta} \zeta \frac{\partial \eta}{\partial \zeta} + 2\upsilon \beta^{1/2} \frac{\partial^2 \eta}{\partial \zeta \partial \tau} + \frac{\partial^2 \eta}{\partial \tau^2} + \left(\frac{L^3}{EI}\right)(m_T + \rho_F A) g \\ &\quad + 2\upsilon^2 C \frac{\partial^2 \eta}{\partial \zeta^2}(\eta - \eta_L) + 2\upsilon^2 C \frac{\partial \xi}{\partial \zeta} \frac{\partial \eta}{\partial \zeta} + \frac{2\upsilon C}{\beta^{1/2}} \frac{\partial \xi}{\partial \tau} \frac{\partial \eta}{\partial \zeta} - \frac{2\upsilon C}{\beta^{1/2}} \frac{\partial^2 \eta}{\partial \zeta^2} \int_\zeta^1 \frac{\partial \xi}{\partial \tau} \mathrm{d}\phi = 0, \end{aligned} \tag{36}$$

where the nondimensional position variable ϕ is defined as

$$\phi = \frac{\psi}{L} \quad (0 \le \phi \le 1) \text{ and } (0 \le \psi \le L). \tag{37}$$

At the fixed end ($\zeta = 0$) of the fluid-tube cantilever system, the geometric boundary conditions for the in-plane displacement and slope, are,

$$\xi(0; \tau) = 0 \quad \text{and} \quad \frac{\partial \xi(0; \tau)}{\partial \zeta} = 0. \tag{38, 39}$$

At the free end ($\zeta = 1$) of the fluid-tube cantilever system, the force boundary conditions for the bending moment and shear force are

$$\frac{\partial^2 \xi(1;\tau)}{\partial \zeta^2} = 0 \quad \text{and} \quad \frac{\partial^3 \xi(1;\tau)}{\partial \zeta^3} = 0. \tag{40, 41}$$

Similarly, at the fixed end ($\zeta = 0$), the geometric boundary conditions for the out-of-plane displacement and slope are

$$\eta(0;\tau) = 0 \quad \text{and} \quad \frac{\partial \eta(0;\tau)}{\partial \zeta} = 0; \tag{42, 43}$$

and at the free end ($\zeta = 1$) of the fluid-tube cantilever system we have

$$\frac{\partial^2 \eta(1;\tau)}{\partial \zeta^2} = 0 \quad \text{and} \quad \frac{\partial^3 \eta(1;\tau)}{\partial \zeta^3} = 0. \tag{44, 45}$$

Equations (35) and (36) include linear, as well as nonlinear terms, a number of which are coupling terms between in-plane and out-of-plane displacements. The significance of the nonlinear terms in the stability of the rotating fluid-tube cantilever system cannot be disregarded without further investigation. However, in the present work, the conditions of stability will be determined for linearized motions of the fluid-tube cantilever, an approximation to the more general nonlinear system. Furthermore, it is assumed that the displacements due to the constant terms, namely the term $2\upsilon^2 C$ in the direction of the y-axis in equation (35) and the term $(L^3/EI)(m_T + \rho_F A)g$ in the direction of the z-axis in equation (36), do not affect the conditions of instability. Hence, leaving out the nonlinear and constant terms in equations (35) and (36) yields the following linear uncoupled non-dimensional differential equations for in-plane and out-of-plane lateral displacements, respectively:

$$\frac{\partial^4 \xi}{\partial \zeta^4} + \upsilon^2 \left[1 + \frac{C^2}{2\beta}(\zeta^2 - 1)\right] \frac{\partial^2 \xi}{\partial \zeta^2} + \frac{\upsilon^2 C^2}{\beta} \zeta \frac{\partial \xi}{\partial \zeta} + 2\upsilon\beta^{1/2} \frac{\partial^2 \xi}{\partial \zeta \partial \tau} + \frac{\partial^2 \xi}{\partial \tau^2} - \frac{\upsilon^2 C^2}{\beta} \xi = 0 \tag{46}$$

and

$$\frac{\partial^4 \eta}{\partial \zeta^4} + \upsilon^2 \left[1 + \frac{C^2}{2\beta}(\zeta^2 - 1)\right] \frac{\partial^2 \eta}{\partial \zeta^2} + \frac{\upsilon^2 C^2}{\beta} \zeta \frac{\partial \eta}{\partial \zeta} + 2\upsilon\beta^{1/2} \frac{\partial^2 \eta}{\partial \zeta \partial \tau} + \frac{\partial^2 \eta}{\partial \tau^2} = 0. \tag{47}$$

5. LINEAR IN-PLANE LATERAL VIBRATIONS

It is assumed that the in-plane lateral vibration of the rotating fluid-tube cantilever system is harmonic in the nondimensional complex frequency

$$\alpha = \alpha_R + \mathrm{i}\alpha_I, \tag{48}$$

where α_R and α_I are the real and imaginary parts of α, respectively. The response of the system is assumed to have the form

$$\xi(\zeta;\tau) = \mathrm{e}^{\mathrm{i}\alpha\tau}\,\mathrm{k}(\zeta) = \mathrm{e}^{\mathrm{i}(\alpha_R + \mathrm{i}\alpha_I)\tau}\,\mathrm{k}(\zeta) = \mathrm{e}^{\mathrm{i}\alpha_R\tau}\mathrm{e}^{-\alpha_I\tau}\,\mathrm{k}(\zeta). \tag{49}$$

The threshold of instability of the system corresponds to $\alpha_I = 0$. The real part α_R becomes the critical nondimensional circular frequency of lateral in-plane vibrations $\omega_{\mathrm{cr/in}}$. Hence,

$$\xi(\zeta;\tau) = \mathrm{e}^{\mathrm{i}\omega_{\mathrm{cr/in}}\tau}\,k(\zeta). \tag{50}$$

Also, in the following, the nondimensional flow velocity in the fluid-tube cantilever system is assumed to be at its critical value, $\upsilon_{\mathrm{cr/in}}$, which renders the imaginary part of α equal to zero. The nondimensional function $k(\zeta)$ must satisfy equation (46) of the in-plane motion of the fluid-tube cantilever system, and the boundary conditions in equations (38)–(41). Following the Galerkin method, the function $k(\zeta)$ is considered to be of the form

$$k(\zeta) = \sum_{r=1}^{N} K_r H_r(\zeta). \tag{51}$$

The function $H_r(\zeta)$ is selected to be the rth normalized eigenfunction of the nonrotating uniform cantilever beam (Bishop & Johnson 1960),

$$H_r(\zeta) = \cosh(\lambda_r \zeta) - \cos(\lambda_r \zeta) - \sigma_r[\sinh(\lambda_r \zeta) - \sin(\lambda_r \zeta)]$$

$$\sigma_r = \frac{\sinh(\lambda_r) - \sin(\lambda_r)}{\cosh(\lambda_r) + \cos(\lambda_r)} \text{ and } \cosh\lambda_r \cos\lambda_r + 1 = 0,\ r = 1, 2, \ldots, N. \tag{52}$$

The coefficient K_r is associated with the rth eigenfunction. The number of modal terms N in equation (51) needs to be large enough, so that, equation (50) adequately represents the motion of the fluid-tube cantilever system. Substitution of equation (51) into equation (50) yields

$$\xi(\zeta; \tau) = \mathrm{e}^{\mathrm{i}\omega_{\mathrm{cr/in}}\tau}\left(\sum_{r=1}^{N} K_r H_r(\zeta)\right). \tag{53}$$

Equation (46) yields

$$\sum_{r=1}^{N} K_r \left\{\left(\lambda_r^4 - \omega_{\mathrm{cr/in}}^2 - \frac{\upsilon_{\mathrm{cr/in}}^2 C^2}{\beta}\right) H_r(\zeta) + \sum_{q=1}^{N}\left[\upsilon_{\mathrm{cr/in}}^2\left(1 - \frac{C^2}{2\beta}\right) c_{rq} + \frac{\upsilon_{\mathrm{cr/in}}^2 C^2}{2\beta}\mathrm{e}_{rq} + \frac{\upsilon_{\mathrm{cr/in}}^2 C^2}{\beta}\mathrm{d}_{rq} + \mathrm{i}\,2\omega_{\mathrm{cr/in}}\upsilon_{\mathrm{cr/in}}\beta^{1/2} b_{rq}\right] H_q(\zeta)\right\} = 0, \tag{54}$$

where

$$b_{rs} = \int_0^1 \frac{\mathrm{d}H_r(\zeta)}{\mathrm{d}\zeta} H_s(\zeta)\,\mathrm{d}\zeta, \quad c_{rs} = \int_0^1 \frac{\mathrm{d}H_r^2(\zeta)}{\mathrm{d}\zeta^2} H_s(\zeta)\,\mathrm{d}\zeta, \quad r, s = 1, 2, \ldots, N, \tag{55, 56}$$

$$d_{rs} = \int_0^1 \zeta\frac{\mathrm{d}H_r(\zeta)}{\mathrm{d}\zeta} H_s(\zeta)\,\mathrm{d}\zeta, \quad e_{rs} = \int_0^1 \zeta^2\frac{\mathrm{d}H_r^2(\zeta)}{\mathrm{d}\zeta^2} H_s(\zeta)\,\mathrm{d}\zeta, \quad r, s = 1, 2, \ldots, N. \tag{57, 58}$$

Formulae for the exact computation of b_{rs} and c_{rs} are given in Gregory & Païdoussis (1966a). Proceeding with the Galerkin method, equation (54) yields

$$K_s\left(\lambda_s^4 - \omega_{\mathrm{cr/in}}^2 - \frac{\upsilon_{\mathrm{cr/in}}^2 C^2}{\beta}\right) + \sum_{r=1}^{N} K_r\left[\upsilon_{\mathrm{cr/in}}^2\left(1 - \frac{C^2}{2\beta}\right) c_{rs} + \frac{\upsilon_{\mathrm{cr/in}}^2 C^2}{2\beta}\mathrm{e}_{rs} + \frac{\upsilon_{\mathrm{cr/in}}^2 C^2}{\beta} d_{rs} + \mathrm{i}2\omega_{\mathrm{cr/in}}\upsilon_{\mathrm{cr/in}}\beta^{1/2} b_{rs}\right] = 0,$$

$$s = 1, 2, \ldots, N. \tag{59}$$

Equations (59) represent a homogeneous linear system of N equations for the N coefficients K_r,

$$[g]\{K\} = \{0\}, \tag{60}$$

where

$$g_{sr} = \left(\lambda_s^4 - \omega_{\mathrm{cr/in}}^2 - \frac{\upsilon_{\mathrm{cr/in}}^2 C^2}{\beta}\right)\delta_{sr} + \upsilon_{\mathrm{cr/in}}^2\left(1 - \frac{C^2}{2\beta}\right)c_{rs} + \frac{\upsilon_{\mathrm{cr/in}}^2 C^2}{2\beta} e_{rs}$$
$$+ \frac{\upsilon_{\mathrm{cr/in}}^2 C^2}{\beta} d_{rs} + \mathrm{i}2\omega_{\mathrm{cr/in}}\upsilon_{\mathrm{cr/in}}\beta^{1/2} b_{rs}, \tag{61}$$

in which δ_{sr} is Kronecker's delta. In order that the coefficients K_r to have nonzero values, the determinant of matrix $[g]$ must be zero, i.e.,

$$\det[g] \equiv \mathscr{Re}(\det[g]) + \mathrm{i}\,\mathscr{Im}(\det[g]) = 0. \tag{62}$$

Equation (62) is the characteristic equation for linear lateral in-plane vibrations of the horizontally rotating fluid-tube cantilever system. In equation (61), the elements g_{sr} of $[g]$ are functions of the critical nondimensional speed of flow $\upsilon_{\mathrm{cr/in}}$, critical nondimensional circular frequency of lateral in-plane vibrations $\omega_{\mathrm{cr/in}}$, speed ratio C, and density ratio β. The determinant det$[g]$, as well as the absolute value abs(det$[g]$) are functions of the same variable set ($\upsilon_{\mathrm{cr/in}}$, $\omega_{\mathrm{cr/in}}$, C, β). For a given set of values C and β, the threshold of instability corresponds to a set of values ($\upsilon_{\mathrm{cr/in}}$, $\omega_{\mathrm{cr/in}}$), which necessarily nullifies the value of abs(det$[g]$), namely,

$$\mathrm{abs}(\det[g(\upsilon_{\mathrm{cr/in}}, \omega_{\mathrm{cr/in}}, C, \beta)]) = 0. \tag{63}$$

If $\upsilon_{\mathrm{cr/in}}$ and $\omega_{\mathrm{cr/in}}$ were plotted in the (C, β)-plane, this would result in two three-dimensional plots, i.e., $\upsilon_{\mathrm{cr/in}}$ would be represented by a surface in the ($\upsilon_{\mathrm{cr/in}}$, C, β)-space. Correspondingly, $\omega_{\mathrm{cr/in}}$ would be represented by a surface in the ($\omega_{\mathrm{cr/in}}$, C, β)-space. However, in this case, the density ratio β was assigned specific values, namely, $\beta = 0{\cdot}2$, 0·5 and 0·8. Let it be recalled that $\beta \in [0, 1]$. Hence, the numerical results for $\upsilon_{\mathrm{cr/in}}$ and $\omega_{\mathrm{cr/in}}$ were plotted as curves in the planes ($\upsilon_{\mathrm{cr/in}}$, C) and ($\omega_{\mathrm{cr/in}}$, C), respectively, for each of the aforementioned β values. The numerical data presented in this work were generated in the computational environment of Mathematica. The data presented in this section were generated using equation (63). An example is demonstrated in Figure 2. In Figure 2(a), contours of the absolute value abs(det$[g]$) are plotted for $(\beta, C) = (0{\cdot}2, 0{\cdot}65)$ in the region $\upsilon \in [17, 24]$ and $\omega \in [84, 160]$. Alternatively, in Figure 2(b), a three-dimensional plot of the inverse of the absolute value Abs(det$[g]$) is created for $(\beta, C) = (0{\cdot}2, 0{\cdot}65)$ in the region $\upsilon \in [16, 24]$ and $\omega \in [80, 160]$. Both Figures 2(a) and 2(b) reveal the location of three potential roots of equation (63). Suitable regions and plotting scales are determined manually by trial and error. Once the location of a potential root is determined, a minimization routine within Mathematica is then employed to yield a more accurate set of values for the $\upsilon_{\mathrm{cr/in}}$ and $\omega_{\mathrm{cr/in}}$.

In order to proceed with the computations, it is important to decide how many modal terms will be retained in equation (51). To this end, the effect of the number of modes N on the critical values ($\upsilon_{\mathrm{cr/in}}$, $\omega_{\mathrm{cr/iin}}$) must be determined. Numerical results were obtained for a range of values of the relative speed ratio C from $C = 0{\cdot}5$ to approximately $C = 0{\cdot}8$, for an increasing number of modes N, starting with $N = 3$ up to $N = 9$ (Panussis 1998). At the same time, the density ratio β was kept equal to 0·2. Results for the 3- and 9-mode approximations are displayed in Figure 3.

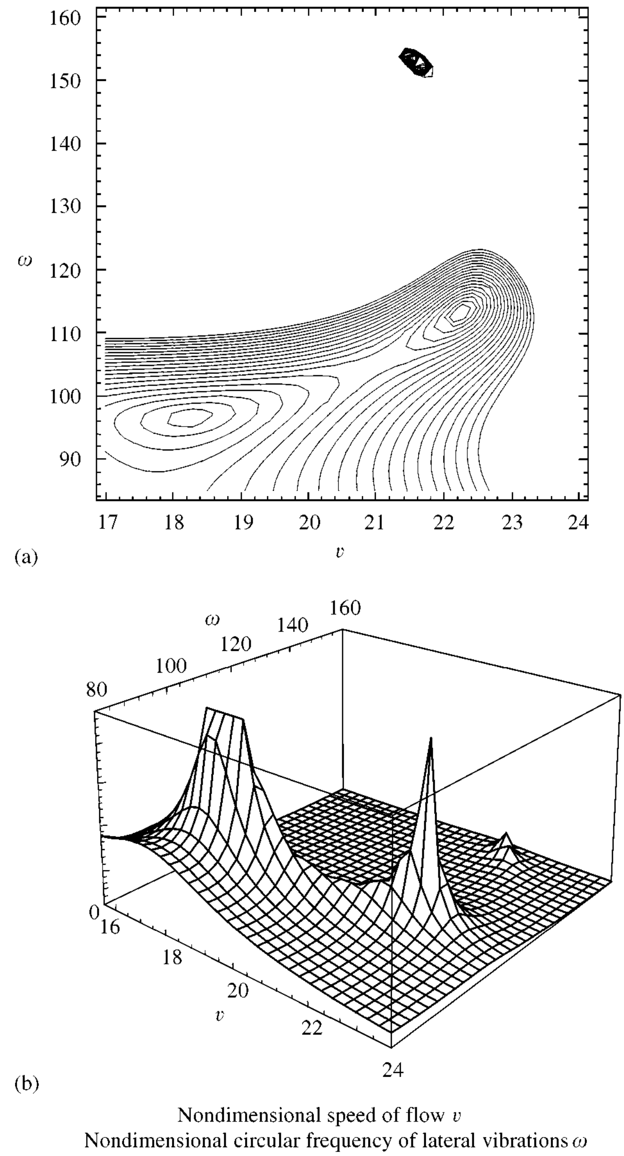

Figure 2. Linear lateral in-plane vibrations with seven Galerkin terms, $\beta = 0{\cdot}2$ and $C = 0{\cdot}65$. (a) A contour plot of abs(det[g]) in the plane (υ, ω) generated by the Mathematica function *ContourPlot*. (b) A three-dimensional plot of $(\text{abs}(\det[g]))^{-1}$ generated by the Mathematica function *Plot3D*.

In the 3-mode Galerkin approximation, the stability curves for $\upsilon_{\mathrm{cr/in}}$ and $\omega_{\mathrm{cr/in}}$ are continuous, without irregularities or multiple root regions. Multiple roots show up for both $\upsilon_{\mathrm{cr/in}}$ and $\omega_{\mathrm{cr/in}}$ in the 4-mode approximation (Panussis 1998). As the number of modes N increases, additional root multiplicity regions develop (Panussis 1998). Also, as the number of modes N increases, the range of the most recently developed multiple roots narrows, whereas earlier multiple roots remain less affected (Panussis 1998). The difference between the 7-mode approximation and the 9-mode approximation is mainly in the second multiplicity region in Figure 3. The latter extends from $C = 0{\cdot}58$ to $C = 0{\cdot}69$ with the 7-mode approximation (Panussis 1998). It extends from $C = 0{\cdot}585$ to $C = 0{\cdot}67$ with the

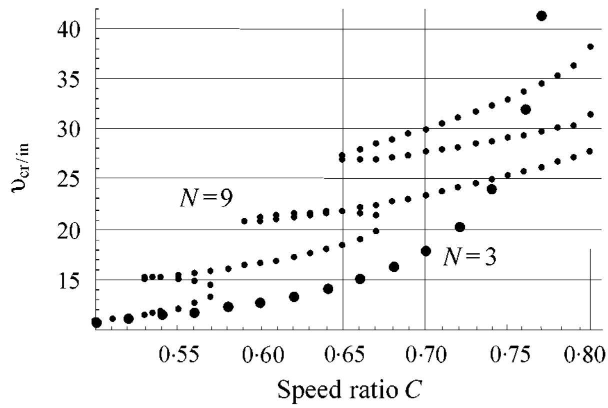

(a) In-plane critical nondimensional speed of flow $\upsilon_{cr/in}$

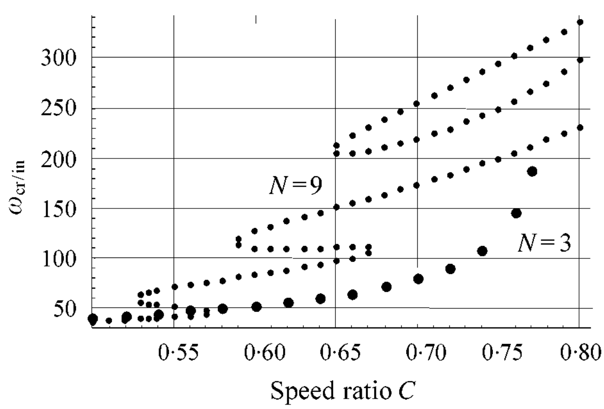

(b) In-plane critical nondimensional circular frequency of lateral vibrations $\omega_{cr/in}$

Figure 3. Stability curves for the horizontally rotating fluid-tube cantilever system, for $\beta = 0{\cdot}2$: the 3-mode ($\bullet\bullet\bullet$) and 9-mode (...) Galerkin approximations are shown.

9-mode approximation in Figure 3. Hence, to use seven terms in the Galerkin approximation for all subsequent numerical calculations, with the understanding that higher C values may require higher modal numbers N. Here the reader is also referred to Païdoussis (1998) for a similar discussion on the nonrotating system.

In another set of numerical results, the in-plane critical nondimensional speed of flow $\upsilon_{cr/in}$ and critical nondimensional circular frequency of lateral vibrations $\omega_{cr/in}$ were computed in a 7-mode approximation. The speed ratio C ranged from $C = 0{\cdot}0$ to approximately $C = 0{\cdot}8$ and the density ratio received values $\beta = 0{\cdot}2$, $0{\cdot}5$ and $0{\cdot}8$ (Figures 4 and 5). Table 1 contains selected numerical data to demonstrate the effect of the number of modal terms N to the quality of the solution for selected β values. The data indicate that higher β values require the inclusion of higher modal terms in the truncated series for equivalent convergence. For example, for $(\beta, C) = (0{\cdot}2, 0{\cdot}5)$, five modal terms are enough to yield a solution with a variation of $0{\cdot}1$, whereas, more than eight modal terms are required in the case $(\beta, C) = (0{\cdot}8, 0{\cdot}5)$.

TABLE 1

The horizontally rotating fluid-tube cantilever in linear in-plane lateral vibrations. The effect of the number of modal terms N on the critical nondimensional speed of flow $\upsilon_{cr/in}$ and the critical nondimensional frequency of lateral vibrations $\omega_{cr/in}$

N	$\beta = 0{\cdot}2$, $\upsilon_{cr/in}$	$C = 0$ $\omega_{cr/in}$	$\beta = 0{\cdot}5$ $\upsilon_{cr/in}$	$C = 0$ $\omega_{cr/in}$	$\beta = 0{\cdot}8$ $\upsilon_{cr/in}$	$C = 0$ $\omega_{cr/in}$
4	5·60124	13·6835	9·4562	28·1971	14·6361	55·8932
5	5·59010	13·7566	9·35931	26·5783	14·188	51·8765
6	5·59379	13·7053	9·32963	26·6624	13·7203	46·586
7	5·59081	13·7253	9·33096	26·4999	13·5168	45·0542
8	5·59221	13·7111	9·32357	26·5414	13·5348	45·1306
N	$\beta = 0{\cdot}2$ $\upsilon_{cr/in}$	$C = 0{\cdot}5$ $\omega_{cr/in}$	$\beta = 0{\cdot}5$ $\upsilon_{cr/in}$	$C = 0{\cdot}5$ $\omega_{cr/in}$	$\beta = 0{\cdot}8$ $\upsilon_{cr/in}$	$C = 0{\cdot}3$ $\omega_{cr/in}$
4	10·8740	37·2737	11·7109	34·0078	15·4179	60·5048
5	10·9067	36·3435	14·1353	56·7265	15·1215	56·0155
6	10·8995	36·381	13·8316	52·3567	14·6949	50·5191
7	10·9005	36·2483	13·7605	51·9441	14·3402	47·6959
8	10·8943	36·2709	13·7588	51·7445	14·3663	47·8712

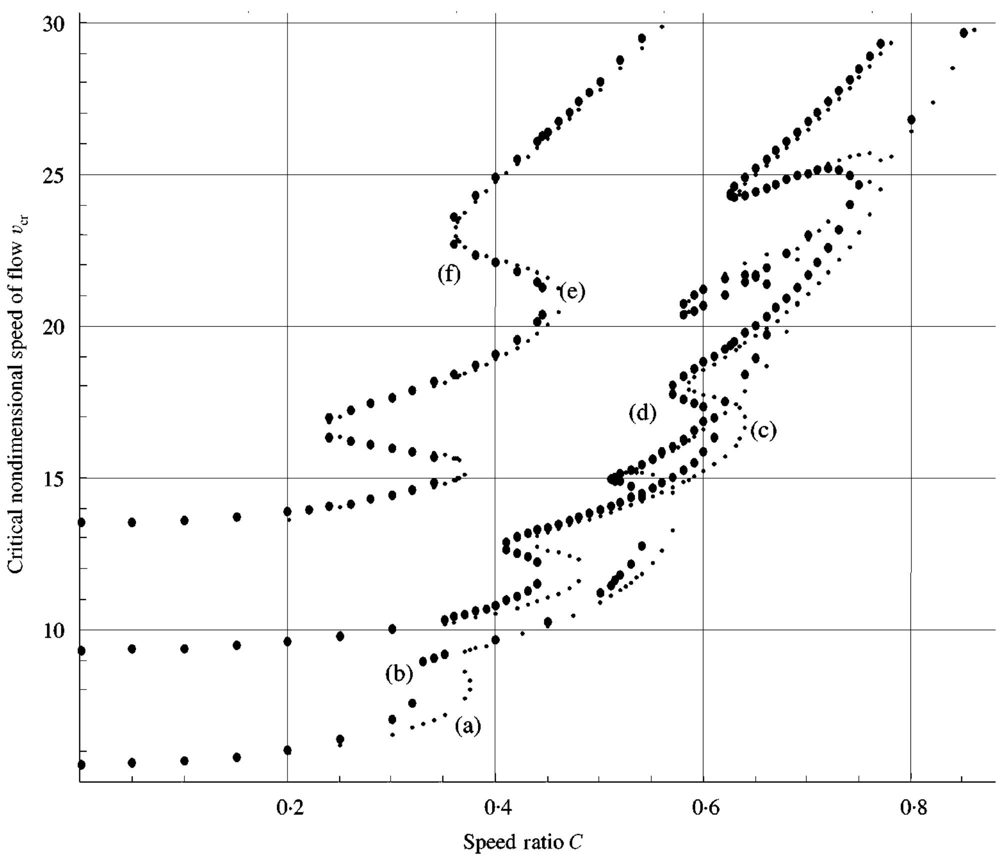

Figure 4. Critical nondimensional speed of flow υ_{cr} for the horizontally rotating fluid-tube cantilever system, using a 7-mode Galerkin approximation. (a) In-plane for density ratio $\beta = 0{\cdot}2$; (b) out-of-plane for $\beta = 0{\cdot}2$; (c) in-plane for $\beta = 0{\cdot}5$; (d) out-of-plane for $\beta = 0{\cdot}5$; (e) in-plane for ratio $\beta = 0{\cdot}8$; (f) out-of-plane for $\beta = 0{\cdot}8$.

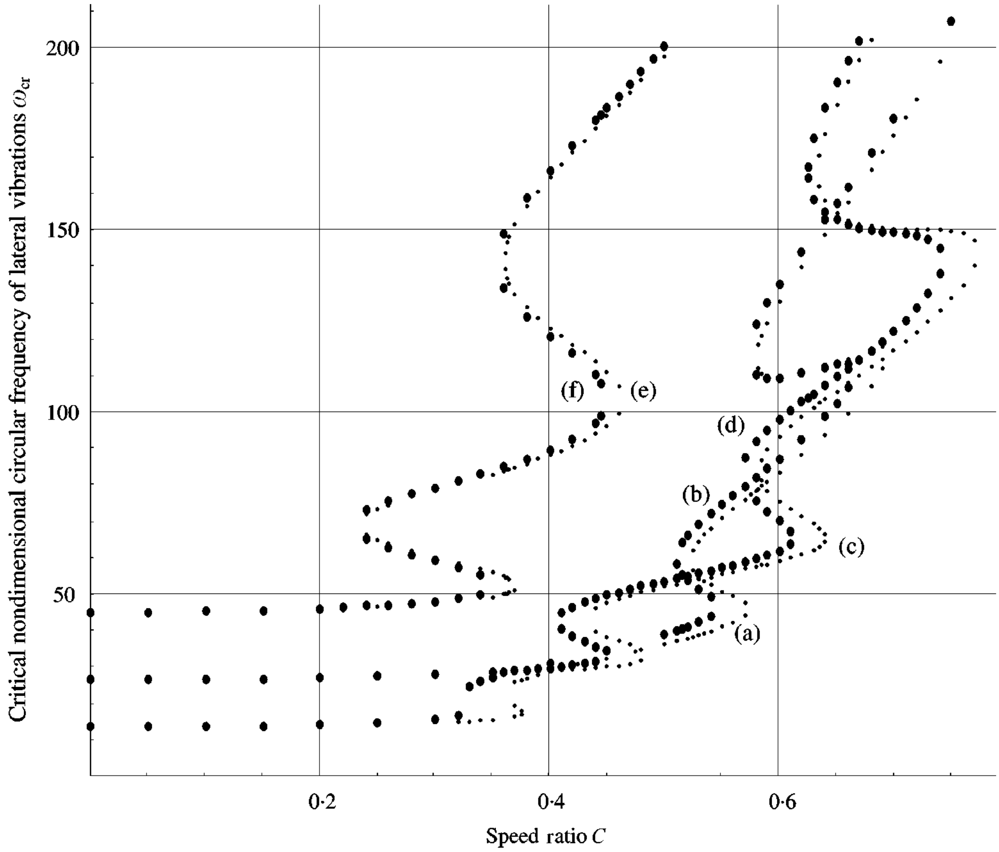

Figure 5. Critical nondimensional circular frequency of lateral vibrations ω_{cr} for the horizontally rotating fluid-tube cantilever system, using a 7-mode Galerkin approximation. (a) In-plane for $\beta = 0{\cdot}2$; (b) out-of-plane for $\beta = 0{\cdot}2$; (c) in-plane for $\beta = 0{\cdot}5$; (d) out-of-plane for $\beta = 0{\cdot}5$; (e) in-plane for $\beta = 0{\cdot}8$; (f) out-of-plane for $\beta = 0{\cdot}8$.

6. LINEAR OUT-OF-PLANE LATERAL VIBRATIONS

As in the case of in-plane lateral vibrations, it is assumed that the horizontally rotating fluid-tube cantilever system vibrates at the out-of-plane critical nondimensional circular frequency of lateral vibrations $\omega_{cr/out}$, and the fluid flows at the out-of-plane critical nondimensional speed of flow $\upsilon_{cr/out}$. In this case, the response of the system is assumed to have the form

$$\eta(\zeta;\tau) = e^{i\omega_{cr/out}\tau} a(\zeta). \tag{64}$$

The function $a(\zeta)$ must be such that equation (64) satisfies the linear out-of-plane differential equation (47), and the boundary conditions in equations (42)–(45). Using the Galerkin method, the function $a(\zeta)$ is considered to be of the form

$$a(\zeta) = \sum_{r=1}^{N} A_r H_r(\zeta). \tag{65}$$

As in the case of in-plane lateral vibrations discussed in the previous section, the function $H_r(\zeta)$ is selected to be the rth normalized eigenfunction of the nonrotating uniform cantilever beam (Bishop and Johnson 1960) in equation (52). The nondimensional coefficient A_r is associated with the rth eigenfunction. The number of modal terms N in equation (65) must be large enough for equation (64) to adequately represent the out-of-plane motion of the system. Substitution of equation (65) into (64) yields

$$\eta(\zeta;\tau) = \mathrm{e}^{\mathrm{i}\omega_{\mathrm{cr/out}}\tau}\left(\sum_{r=1}^{N} A_r H_r(\zeta)\right). \tag{66}$$

Substitution in equation (47) yields

$$\sum_{r=1}^{N} A_r \left\{\left(\lambda_r^4 - \omega_{\mathrm{cr/out}}^2\right)H_r(\zeta) + \sum_{q=1}^{N}\left[\upsilon_{\mathrm{cr/out}}^2\left(1-\frac{C^2}{2\beta}\right)c_{rq} + \frac{\upsilon_{\mathrm{cr/out}}^2 C^2}{\beta}\,\mathrm{d}_{rq} + \frac{\upsilon_{\mathrm{cr/out}}^2 C^2}{2\beta}\,\mathrm{e}_{rq} + \mathrm{i}\,2\omega_{\mathrm{cr/out}}\,\upsilon_{\mathrm{cr/out}}\,\beta^{1/2} b_{rq}\right]H_q(\zeta)\right\} = 0, \tag{67}$$

and hence

$$A_s(\lambda_s^4 - \omega_{\mathrm{cr/out}}^2) + \sum_{r=1}^{N} A_r\left[\upsilon_{\mathrm{cr/out}}^2\left(1-\frac{C^2}{2\beta}\right)c_{rs} + \frac{\upsilon_{\mathrm{cr/out}}^2 C^2}{2\beta}\,e_{rs} + \frac{\upsilon_{\mathrm{cr/out}}^2 C^2}{\beta}\,d_{rs} + \mathrm{i}2\omega_{\mathrm{cr/out}}\,\upsilon_{\mathrm{cr/out}}\,\beta^{1/2} b_{rs}\right] = 0,$$
$$s = 1, 2, \ldots, N. \tag{68}$$

Equations (68) represent a homogeneous linear system of N equations in N coefficients A_r,

$$[f]\{A\} = \{0\}, \tag{69}$$

where

$$f_{sr} = (\lambda_s^4 - \omega_{\mathrm{cr/out}}^2)\delta_{sr} + \upsilon_{\mathrm{cr/out}}^2\left(1-\frac{C^2}{2\beta}\right)c_{rs} + \frac{\upsilon_{\mathrm{cr/out}}^2 C^2}{2\beta}\,e_{rs} + \frac{\upsilon_{\mathrm{cr/out}}^2 C^2}{\beta}\,d_{rs} + \mathrm{i}2\omega_{\mathrm{cr/out}}\,\upsilon_{\mathrm{cr/out}}\,\beta^{1/2} b_{rs}. \tag{70}$$

δ_{sr} being Kronecker's delta. For the coefficients A_r to have nonzero values, the determinant of matrix $[f]$ must be zero, i.e.,

$$\det[f] \equiv \mathscr{Re}(\det[f]) + \mathrm{i}\,\mathscr{Im}(\det[f]) = 0. \tag{71}$$

Equation (71) is the characteristic equation for linear out-of-plane lateral vibrations of the horizontally rotating fluid-tube cantilever system. Following the same reasoning as in the case of the linear in-plane vibrations, for given values of C and β, the threshold of instability corresponds to a critical set ($\upsilon_{\mathrm{cr/out}}$, $\omega_{\mathrm{cr/out}}$), which nullifies the value of abs(det$[f]$), namely,

$$\mathrm{abs}(\det[f(\upsilon_{\mathrm{cr/out}}, \omega_{\mathrm{cr/out}}, C, \beta)]) = 0. \tag{72}$$

The critical values of the out-of-plane nondimensional speed of flow $\upsilon_{\mathrm{cr/out}}$ and nondimensional circular frequency of lateral vibrations $\omega_{\mathrm{cr/out}}$ were computed using seven modal terms for the speed ratio C ranging from $C = 0{\cdot}0$ to approximately $C = 0{\cdot}8$ and density ratio $\beta = 0{\cdot}2$, $0{\cdot}5$ and $0{\cdot}8$. The results are presented in Figures 4 and 5. The effect of the number of modes N on the critical values ($\upsilon_{\mathrm{cr/out}}$, $\omega_{\mathrm{cr/out}}$) is partially demonstrated in Tables 2 and 3.

TABLE 2
The horizontally rotating fluid-tube cantilever in linear out-of-plane lateral vibrations. The effect of the number of modal terms N on the critical nondimensional speed of flow $\upsilon_{cr/out}$ and critical nondimensional circular frequency of lateral vibrations $\omega_{cr/out}$

N	$\beta = 0{\cdot}2$ $\upsilon_{cr/out}$	$C = 0$ $\omega_{cr/out}$	$\beta = 0{\cdot}5$ $\upsilon_{cr/out}$	$C = 0$ $\omega_{cr/out}$	$\beta = 0{\cdot}8$ $\upsilon_{cr/out}$	$C = 0$ $\omega_{cr/out}$
2	5·41891	14·0462	8·24857	11·37	9·76314	9·01654
3	5·59747	14·0798	9·47306	29·4416	11·1012	27·3969
4	5·60124	13·6835	9·45620	28·1971	14·5223	55·8932
5	5·5901	13·7566	9·35931	26·5783	14·188	51·8765
6	5·59379	13·7053	9·32963	26·6624	13·7203	46·586
7	5·59081	13·7253	9·33096	26·4999	13·5168	45·0542
8	5·59221	13·7111	9·32357	26·5414	13·5348	45·1306
N	$\beta = 0{\cdot}2$ $\upsilon_{cr/out}$	$C = 0{\cdot}5$ $\omega_{cr/out}$	$\beta = 0{\cdot}5$ $\upsilon_{cr/out}$	$C = 0{\cdot}5$ $\omega_{cr/out}$	$\beta = 0{\cdot}8$ $\upsilon_{cr/out}$	$C = 0{\cdot}3$ $\omega_{cr/out}$
2	8·85269	20·7552	15·8669	14·2362	10·7858	9·2501
3	11·0311	43·3031	11·529	35·8129	11·679	28·1263
4	11·1291	40·0175	13·2913	41·5854	15·4723	60·7569
5	11·2265	39·1201	14·3233	58·889	15·2101	56·4993
6	11·2095	39·1277	14·0381	54·3386	14·8174	51·1741
7	11·2186	39·0138	13·9468	53·6934	14·4386	48·1169
8	11·2078	39·0189	13·9514	53·5701	14·4642	48·2944

7. IN-PLANE VERSUS OUT-OF-PLANE LINEAR LATERAL VIBRATIONS

Comparison between the linear in-plane and out-of-plane lateral vibration types in Figures 4 and 5 reveals that for a specific set of values for β and C, the conditions of instability in the out-of-plane type in most cases correspond to higher υ_{cr} and ω_{cr} values than in the in-plane type. Namely, the horizontally rotating fluid-tube cantilever system is less stiff when it vibrates in-plane than out-of-plane. This is evident in the single valued regions of the stability curves, i.e., regions without multiplicity. In the multiplicity regions, one must distinguish the lower and upper from the middle segment of the multiplicity bend. In the lower and upper segments, the in-plane υ_{cr} and ω_{cr} values are lower that the out-of-plane ones. In the middle segment, the opposite is true. The difference in the results between in-plane and out-of-plane is considerably reduced for the density ratio $\beta = 0{\cdot}8$ in Figure 4(e,f) and Figure 5(e, f). However, for a given density ratio β, the corresponding in-plane stability curves υ_{cr} and ω_{cr} are always located to the right of the out-of-plane ones. Hence, a rotating fluid-tube cantilever system with a given density ratio β and flow velocity υ can in theory become unstable, firstly out-of-plane at a lower speed ratio C and subsequently in-plane at a higher C value.

It should be recalled that the numerical results in this work were obtained by considering the two types of lateral vibrations to be of small amplitude, uncoupled and linear. In Table 1, the in-plane results obtained with $N = 8$ vary as follows, when compared with those obtained with $N = 7$: for $(\beta, C) = (0{\cdot}2, 0{\cdot}5)$, by $-0{\cdot}06$ and 0·06%, for $\upsilon_{cr/in}$ and $\omega_{cr/in}$, respectively, for $(\beta, C) = (0{\cdot}5, 0{\cdot}5)$, by $-0{\cdot}01$ and $-0{\cdot}38$%, respectively; for $(\beta, C) = (0{\cdot}8, 0{\cdot}3)$, by 0·18 and 0·37%, respectively. In Table 2, the out-of-plane results obtained with $N = 8$ vary as follows, when compared with those obtained with $N = 7$: for $(\beta, C) = (0{\cdot}2, 0{\cdot}5)$, by $-0{\cdot}10$ and 0·01%, for $\upsilon_{cr/out}$ and $\omega_{cr/out}$, respectively: for $(\beta, C) = (0{\cdot}5, 0{\cdot}5)$, by 0·03 and $-0{\cdot}23$%, respectively; for $(\beta, C) = (0{\cdot}8, 0{\cdot}3)$, by 0·18 and 0·37%, respectively. In row $N = 7$ in Table 2, the value of the out-of-plane critical

TABLE 3

The horizontally rotating fluid-tube cantilever in linear out-of-plane lateral vibrations. The effect of the number of modal terms N on the error (%) in the computation of the critical nondimensional speed of flow $\upsilon_{cr/out}$ and critical nondimensional circular frequency of lateral vibrations $\omega_{cr/out}$. Data are from Table 2

N	$\beta = 0{\cdot}2$ $(\Delta\upsilon_{cr}/\upsilon_{cr})_{out}$	$C = 0$ $(\Delta\omega_{cr}/\omega_{cr})_{out}$	$\beta = 0{\cdot}5$ $(\Delta\upsilon_{cr}/\upsilon_{cr})_{out}$	$C = 0$ $(\Delta\omega_{cr}/\omega_{cr})_{out}$	$\beta = 0{\cdot}8$ $(\Delta\upsilon_{cr}/\upsilon_{cr})_{out}$	$C = 0$ $(\Delta\omega_{cr}/\omega_{cr})_{out}$
3	3·295 (%)	0·239 (%)	14·845 (%)	158·941 (%)	13·705 (%)	203·852 (%)
4	0·067	−2·815	−0·178	−4·227	30·817	104·013
5	−0·198	0·534	−1·025	−5·741	−2·302	−7·186
6	0·066	−0·373	−0·317	0·316	−3·296	−10·198
7	−0·053	0·146	0·014	−0·609	−1·483	−3·288
8	0·025	−0·103	−0·079	0·157	0·133	0·170
N	$\beta = 0{\cdot}2$ $(\Delta\upsilon_{cr}/\upsilon_{cr})_{out}$	$C = 0{\cdot}5$ $(\Delta\omega_{cr}/\omega_{cr})_{out}$	$\beta = 0{\cdot}5$ $(\Delta\upsilon_{cr}/\upsilon_{cr})_{out}$	$C = 0{\cdot}5$ $(\Delta\omega_{cr}/\omega_{cr})_{out}$	$\beta = 0{\cdot}8$ $(\Delta\upsilon_{cr}/\upsilon_{cr})_{out}$	$C = 0{\cdot}3$ $(\Delta\omega_{cr}/\omega_{cr})_{out}$
3	24·607 (%)	108·637 (%)	−27·339 (%)	151·562 (%)	8·281 (%)	204·065 (%)
4	0·888	−7·587	15·286	16·118	32·480	116·015
5	0·875	−2·243	7·764	41·610	−1·695	−7·008
6	−0·151	0·019	−1·991	−7·727	−2·582	−9·425
7	0·081	−0·291	−0·65	−1·187	−2·556	−5·974
8	−0·096	0·013	0·033	−0·230	0·177	0·369

nondimensional speed of flow $\upsilon_{cr/out}$ is 2·98% higher than the in-plane value in Table 1, when $(\beta, C) = (0{\cdot}2, 0{\cdot}5)$. The corresponding percentage increase for the critical nondimensional circular frequency of vibration $\omega_{cr/out}$ is 7·56%. For $(\beta, C) = (0{\cdot}5, 0{\cdot}5)$, the numbers are 1·37 and 3·77%, respectively, and for $(\beta, C) = (0{\cdot}8, 0{\cdot}3)$, they are 0·50 and 0·51%, respectively. These results show that, for the cited examples, the difference in the critical values υ_{cr} and ω_{cr} between the out-of-plane and in-plane types is reduced as the density ratio β is increased. Namely, the flow of relatively denser fluids reduces the effect of the additional term $[-(\upsilon^2_{cr/in}C^2/\beta)\xi]$ in equation (46). However, for $(\beta, C) = (0{\cdot}8, 0{\cdot}3)$, the difference between the out-of-plane and in-plane results is comparable with the difference between the results obtained with seven modal terms and those obtained with eight terms. This is an indication that for higher β values, a larger number N, i.e., higher-order modal terms are required to obtain reliable results. The latter can be seen in Table 3, which contains the error in the computation of the out-of-plane critical nondimensional speed of flow and critical nondimensional circular frequency of lateral vibrations. The data in Table 3 were computed using the results from Table 2. A similar effect was observed with regard to the speed ratio C as the modal number N increases (Panussis 1998). Therefore, higher-order modal terms affect the shape of the stability curves in regions of higher C values more than in regions of lower C values.

8. ROTATING VERSUS NONROTATING FLUID-TUBE CANTILEVER SYSTEM

The in-plane and out-of-plane values of the critical nondimensional speed of flow υ_{cr} and critical nondimensional circular frequency of lateral vibrations ω_{cr}, represented by the stability curves in Figures 4 and 5, respectively, for the rotating system are higher than in

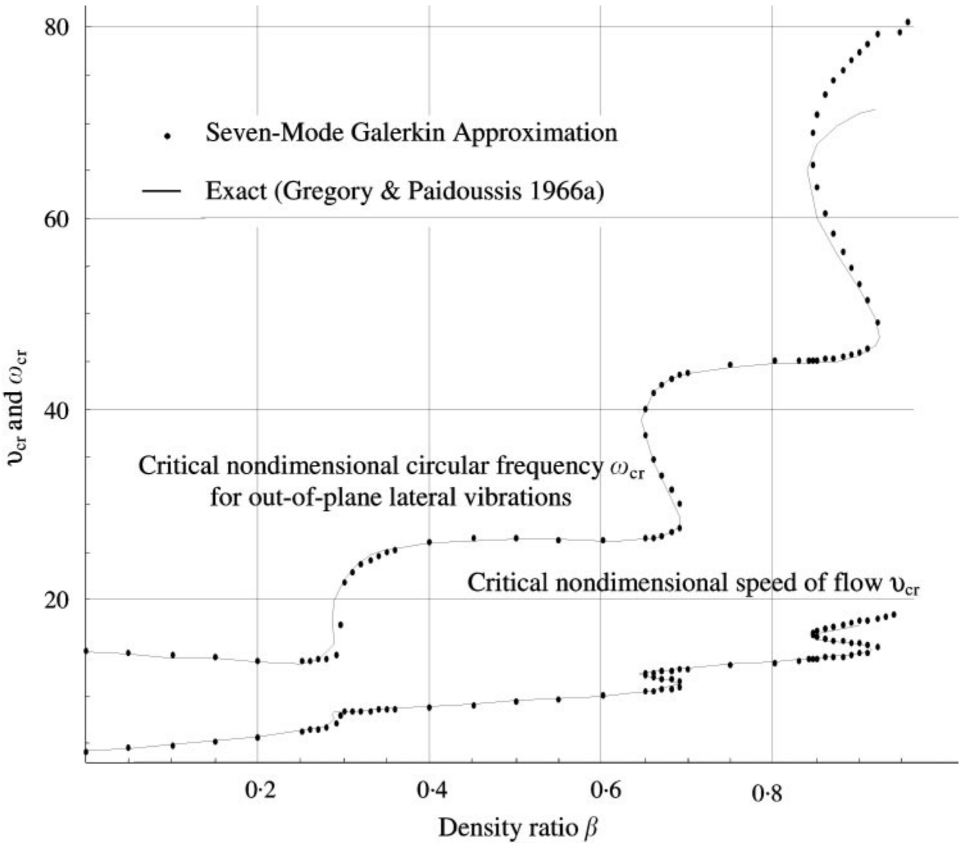

Figure 6. Stability curves for out-of-plane lateral vibrations for the horizontal nonrotating fluid-tube cantilever system (speed ratio $C \equiv \Omega_0 L/U = 0$): $\cdots$, 7-mode Galerkin approximation; ——, exact results adapted from Gregory & Paidoussis (1966a).

the nonrotating case $\Omega_0 = 0 (C \equiv \Omega_0 L/U = 0)$. In the case $\Omega_0 = 0 (C = 0)$, the linear in-plane differential equation (46) and the out-of-plane equation (47) yield the same equation of motion

$$\frac{\partial^4 \xi}{\partial \zeta^4} + \upsilon^2 \frac{\partial^2 \xi}{\partial \zeta^2} + 2\upsilon\beta^{1/2} \frac{\partial^2 \xi}{\partial \zeta \partial \tau} + \frac{\partial^2 \xi}{\partial \tau^2} = 0. \tag{73}$$

Equation (73) represents the nondimensional form of the well-known differential equation of motion of the nonrotating fluid-tube cantilever without internal or external damping (Niordson 1953; Benjamin 1961a; Gregory & Païdoussis 1966a). Tables 1 and 2 contain the critical values (υ_{cr}, ω_{cr}) for the cases (β, C) = (0·2, 0) and (β, C) = (0·5, 0) for $N = 7$ modal terms; namely, (υ_{cr}, ω_{cr}) = (5·59081, 13·7253) and (υ_{cr}, ω_{cr}) = (9·33096, 26·4999), respectively. These results can also be found in the stability curves in Figures 4 and 5.

Figure 6 compares the results between the present work and the analytical solution for the nonrotating fluid-tube cantilever system (Gregory & Paidoussis 1966a). Up to approximately $\beta = 0{\cdot}8$, the 7-mode Galerkin approximation compares well with the exact solution. For values of the density ratio β higher than 0·8, a deviation of the numerical results from the exact solution is noted, both for the critical nondimensional speed of flow υ_{cr} and the critical nondimensional circular frequency of lateral vibrations ω_{cr}. It was shown (Gregory & Païdoussis 1966a) that the multiplicity in the regions $\beta = 0{\cdot}28$ and $0{\cdot}65$ is due to the behavior of modal terms of higher order. In this case, the effect only becomes evident when an adequate number of modal terms are included. A similar observation can be made in the case of the rotating fluid-tube cantilever system based on the numerical results in Panussis (1998).

9. THE ROTATING FLUID-TUBE CANTILEVER VERSUS THE ROTATING UNIFORM CANTILEVER WITHOUT FLOW

The numerical results for the critical nondimensional circular frequency of out-of-plane lateral vibrations $\omega_{cr/out}$ of the horizontally rotating fluid-tube cantilever system are compared with the corresponding critical values $\omega_{cr/nf}$ of a rotating uniform cantilever beam without internal flow. For the out-of-plane case, the element f_{sr} in the coefficient matrix $[f]$, is given in equation (70). The nondimensional angular speed of rotation η_0 of the rotating uniform cantilever beam has been expressed in terms of the out-of-plane nondimensional speed of flow υ_{out} and the speed ratio C in equation (A3). At the onset of out-of-plane lateral instability, the nondimensional speed of flow υ_{out} receives the critical value $\upsilon_{cr/out}$ and equation (A3) yields

$$\eta_0 = \upsilon_{cr/out} C \left(\frac{1}{\beta} - 1 \right)^{1/2}. \tag{74}$$

Substitution for $\upsilon_{cr/out} C$ from equation (74) into equation (70) yields

$$f_{sr} = (\lambda_s^4 - \omega_{cr/out}^2)\delta_{sr} + \left(\upsilon_{cr/out}^2 - \frac{\eta_0^2}{2(1-\beta)} \right) c_{rs} + \frac{\eta_0^2}{2(1-\beta)} e_{rs} + \frac{\eta_0^2}{(1-\beta)} d_{rs} + \mathrm{i}2\omega_{cr/out}\upsilon_{cr/out}\beta^{1/2} b_{rs}. \tag{75}$$

In the case of the rotating uniform cantilever beam without flow, the nondimensional speed of flow υ is no longer present in the problem. In that case, the critical out-of-plane nondimensional speed of flow $\upsilon_{cr/out}$–is no longer present in equation (75). The latter yields

$$f_{sr/nf} = (\lambda_s^4 - \omega_{cr/nf}^2)\delta_{sr} - \frac{\eta_0^2}{2(1-\beta)} c_{rs} + \frac{\eta_0^2}{2(1-\beta)} e_{rs} + \frac{\eta_0^2}{(1-\beta)} d_{rs}. \tag{76}$$

The characteristic equation for linear out-of-plane lateral vibrations of the horizontally rotating tubular cantilever without flow is

$$\det[f_{nf}] = 0. \tag{77}$$

Equation (77) was solved numerically with a 7-mode approximation for the critical nondimensional circular frequency of out-of-plane lateral vibrations without internal flow $\omega_{cr/nf}$ in the range $\eta_0 = \{0, 1, 2, \ldots, 12\}$ and for density ratio values $\beta = \{0{\cdot}0001, 0{\cdot}2, 0{\cdot}5, 0{\cdot}8\}$ (Figure 7 and Table 4). The presence of nonflowing fluid inside the rotating uniform cantilever tube affects the threshold of instability of the system. The numerical results show that, when maintaining the nondimensional angular speed of rotation η_0 constant, the higher the density ratio β, the higher the critical $\omega_{cr/nf}$ value.

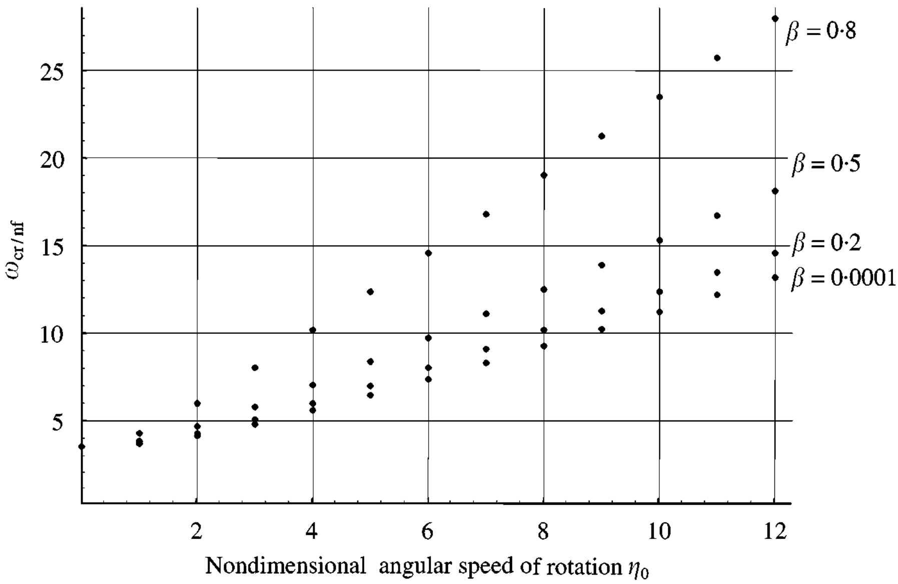

Figure 7. The critical nondimensional circular frequency $\omega_{cr/nf}$ for out-of-plane lateral vibrations of a rotating uniform cantilever tube containing a nonflowing fluid, using a 7-mode Galerkin approximation for the values of the density ratio $\beta = \{0{\cdot}0001, 0{\cdot}2, 0{\cdot}5, 0{\cdot}8\}$. Data are from Table 4.

TABLE 4

The exact critical nondimensional circular frequency $\omega_{cr/nf}$ of out-of-plane lateral vibrations of a rotating uniform cantilever linear Euler–Bernoulli beam in terms of the nondimensional angular speed of rotation $\eta_0 = \Omega_0 L^2 (m_T/EI)^{1/2}$, adapted from Du *et al.* (1994). The third column contains the corresponding $\omega_{cr/nf}$ values using the approximate formula in Peters (1973). The last four columns contain the corresponding $\omega_{cr/nf}$ values of a rotating uniform cantilever tube containing a nonflowing fluid, computed numerically using a 7-mode Galerkin approximation for different values of the density ratio $\beta = \rho_F A/(m_T + \rho_F A)$

	Rotating uniform cantilever beam		Rotating uniform cantilever tube containing nonflowing fluid with density ratio $\beta = \rho_F A/(m_T + \rho_F A)$			
η_0	$(\omega_{cr/nf})_{exact}$	$(\omega_{cr/nf})_{approximate}$	$(\omega_{cr/nf})_{approximate}$ using 7-mode Galerkin			
	(Du *et al.* 1994)	(Peters 1973)	$\beta = 0{\cdot}0001$	$\beta = 0{\cdot}2$	$\beta = 0{\cdot}5$	$\beta = 0{\cdot}8$
0	3·51602	3·516000	3·51602	3·51602	3·51602	3·51602
1	3·68165	3·681615	3·68166	3·72185	3·83984	4·27794
2	4·13732	4·137084	4·1374	4.27794	4·67317	5·98588
3	4·79728	4·796436	4·7974	5·06477	5·78918	8·02347
4	5·58500	5·583156	5·5852	5·98588	7·04398	10·1719
5	6·44954	6·446493	6·4498	6·98291	8·36733	12·3629
6	7·36037	7·356137	7·3607	8·02347	9·72617	14·5732
7	8·29964	8·294398	8·3001	9·08978	11·1045	16·7936
8	9·25684	9·250850	9·2575	10·1719	12·4943	19·0202
9	10·2257	10·219212	10·2266	11·2641	13·8913	21·2511
10	11·2023	11·195597	11·2035	12·3629	15·293	23·4851
11	12·1843	12·177535	12·1859	13·4664	16·698	25·7218
12	13·1702	13·163413	13·1721	14·5732	18·1055	27·9608

10. CONCLUSIONS

This work investigated the conditions for instability of a horizontally rotating fluid-tube cantilever system, a hybrid of the fixed fluid-tube cantilever and the rotating uniform cantilever beam without inner flow. The numerical analysis was based on a linear approximation using the Galerkin method. The quality of the convergence does not improve uniformly across the range of values of the speed ratio C, or across the range of values of the density ratio β. As the number of modal terms N increases, the convergence of the solution first improves for the lower C values and later for the higher ones. So is the case for the density ratio β also.

In the case of linear in-plane, as well as out-of-plane lateral vibrations, the numerical results show that the horizontal rotational motion has a stiffening effect on the fluid-tube cantilever system. However, in both cases, values $C < 0{\cdot}2$ do not considerably affect the threshold of instability of the fluid-tube system. For a given speed ratio C, higher density ratios β yield higher critical values, depending on the particular set (C, β). For a given set (C, β), the critical nondimensional values in the in-plane type are lower than in the out-of-plane type, the difference reducing as the density ratio β increases. The former is true throughout, except for the middle segment of the multiplicity folds in the stability curves, where the opposite is true.

The results found in the present work were compared to the analytical solution for the nonrotating fluid-tube cantilever system. For up to approximately $\beta = 0{\cdot}8$, the 7-mode approximation compares well with the exact solution. For values β higher than 0·8, the approximate solution yields critical values higher than the exact solution.

The approximate theory developed in this work gave similar results with an exact and an earlier approximate solution, in the case of the rotating uniform cantilever beam without internal flow. The stability of the system is affected by the presence of nonflowing fluids inside the rotating uniform cantilever. For a given nondimensional angular speed of rotation, higher β values yield higher critical nondimensional circular frequency of lateral vibrations.

REFERENCES

BENJAMIN, T. B. 1961a Dynamics of a system of articulated pipes conveying fluid: I. Theory. *Proceedings of the Royal Society* (*London*) A **261,** 457–486.

BENJAMIN, T. B. 1961b Dynamics of a system of articulated pipes conveying fluid: II. Experiments. *Proceedings of the Royal Society* (*London*) A **261,** 487–499.

BISHOP, R. E. D. & JOHNSON, D. C. 1960 *The Mechanics of Vibration*. Cambridge: Cambridge University Press.

BLEVINS, R. D. 1990 *Flow-Induced Vibration*. 2nd ed. New York: Van Nostrand Reinhold.

CHEN, S. S. 1987 *Flow-Induced Vibration of Circular Structures*. Washington: Hemisphere.

CURRIE, I. G. 1974 *Fundamental Mechanics of Fluids*. New York: McGraw-Hill.

DU, H., LIM, M. K. & LIEW, K. M. 1994 A power series solution for vibration of a rotating Timoshenko beam. *Journal of Sound and Vibration* **175,** 505–523.

GREGORY, R. W. & PAÏDOUSSIS, M. P. 1966a Unstable oscillation of tubular cantilevers conveying fluid, Part I. Theory. *Proceedings of the Royal Society* (*London*) A **293,** 512–527.

GREGORY, R. W. & PAÏDOUSSIS, M. P. 1966b Unstable oscillation of tubular cantilevers conveying fluid, Part II. Experiments. *Proceedings of the Royal Society* (*London*) A **293,** 528-542.

HOUBOLT, J. C. & BROOKS, G. W. 1957 Differential equations of motion for combined flapwise bending, chordwise bending, and torsion of twisted nonuniform rotor blades. *NACA TN 3905*. Langley Aeronautical Laboratory, Langley Field, VA, U.S.A.

JOHNSON, W. 1994 *Helicopter Theory*. New York: Dover Publications.

NIORDSON, F. I. N. 1953 Vibrations of a cylindrical tube containing flowing fluid. *Transactions of the Royal Institute of Technology*, No. 73. Stockholm, Sweden.

O'NEIL, P. V. 1991. *Advanced Engineering Mathematics*. Belmont: Wadsworth Publishing Company.

PAÏDOUSSIS, M.P. 1970 Dynamics of tubular cantilevers conveying fluid. *Journal Mechanical Engineering Science* **12,** 85–103.

PAÏDOUSSIS, M. P. & ISSID, N. T. 1974 Dynamic stability of pipes conveying fluid. *Journal of Sound and Vibration* **33,** 267–294.
PAÏDOUSSIS, M. P. 1987 Flow-induced instabilities of cylindrical structures. *Applied Mechanics Reviews* **40,** 163–175.
PAÏDOUSSIS, M. P. 1993 1992 CALVIN RICE LECTURE: Some curiosity-driven research in fluid structure interactions and its current applications. *ASME Journal of Pressure Vessel Technology* **115,** 2–14.
PAÏDOUSSIS, M. P. 1998 *Fluid–Structure Interactions: Slender Structures and Axial Fluid*, Vol. 1. London: Academic Press.
PANUSSIS, D. A. & DIMAROGONAS, A. D. 1997 Stability of a horizontally rotating fluid-tube cantilever. *Proceedings, ASME 4th International Symposium on Fluid-Structure Interactions, Aeroelasticity, Flow-Induced Vibration and Noise*, AD **53,** 47–56. New York: ASME.
PANUSSIS, D. A. 1998 Stability of an interactive fluiad-tube cantilever system in a horizontal rotational motion. D.Sc. Dissertation, Department of Mechanical Engineering, Washington University, Sever Institute of Technology, Saint Louis, Missouri, U.S.A.
PETERS, D. A. 1973 An approximate solution for the free vibrations of rotating uniform cantilever beams. NASA TM X-62,299. Ames Research Center and U.S. Army Air Mobility R&D Laboratory, Moffett Field, CA, U.S.A.

APPENDIX A

An approximate closed-form expression for the critical nondimensional circular frequency of out-of-plane lateral vibration $\omega_{\mathrm{cr/nf}}$ of a rotating flexible uniform cantilever beam without internal flow is given by Peters (1973):

$$\omega^2_{\mathrm{cr/nf}} = \eta_0 + 12{\cdot}3623 + \frac{3\sqrt{2}}{\pi}\eta_0^{1/2}\arctan\left[\frac{0{\cdot}19334\pi\eta_0^{1/2}}{3\sqrt{2}}\right]. \tag{A1}$$

The value of function arctan[ ] must be returned in radians.

In equation (A1) η_0 is the nondimensional speed of rotation of the cantilever beam, in this case a tubular beam, defined as (Peters 1973)

$$\eta_0 = \Omega_0 L^2\left(\frac{m_T}{EI}\right)^{1/2}. \tag{A2}$$

Introducing equations (32)–(34) into equation (A2) yields

$$\eta_0 = \upsilon C\left(\frac{1}{\beta} - 1\right)^{1/2}. \tag{A3}$$

APPENDIX B: NOMENCLATURE

A	cross-sectional area of the flow
$\{A\}$	out-of-plane non-dimensional Galerkin coefficient vector
$a(\zeta)$	response function for out-of-plane lateral vibrations
$[b]$	coefficient matrix of size $N \times N$
C	speed ratio: the ratio of cantilever tip speed (tangential velocity) to fluid radial velocity
$[c]$	coefficient matrix of size $N \times N$
D	internal diameter of the rotating fluid-tube cantilever
$[d]$	coefficient matrix of size $N \times N$
E	modulus of elasticity of the tube material
$\mathbf{e}_n(x; t)$	unit vector normal to the deflected elastic axis of the tubular cantilever
$\mathbf{e}_t(x; t)$	unit vector tangent to the deflected elastic axis of the tubular cantilever
$[e]$	coefficient matrix of size $N \times N$
$[f]$	Galerkin matrix of size $N \times N$
$[g]$	Galerkin matrix of size $N \times N$
g	acceleration due to gravity
$\{H(\zeta)\}$	normalized eigenfunction vector of the flexible cantilever beam

I	second moment of inertia of the axisymmetric cross section of the fluid-tube cantilever with respect to one of the axes of symmetry
i	(i) complex number unit; (ii) Index
$\{K\}$	in-plane non-dimensional Galerkin coefficient vector
$k(\zeta)$	response function for in-plane lateral vibrations
L	length of the tube
m_T	mass per unit length of the tube portion of the fluid-tube cantilever
N	number of modes
q_i	generalized coordinate
q	index
$R(x; t)$	total curvature of the displaced elastic axis.
$\mathbf{r}(x; t)$	position vector of the displaced fluid-tube element
r	index
s	(*i*) tube length measured on the deflected elastic axis; (ii) index
$T_{\mathrm{F}}(t)$	kinetic energy of the fluid contained at any time within the tube
$\dot{T}_{\mathrm{flux}}(t)$	efflux of kinetic energy through the control surface
$T_{\mathrm{in}}(t)$	inflow of kinetic energy through the control surface
$T_{\mathrm{out}}(t)$	outflow of kinetic energy through the control surface
$T_T(t)$	kinetic energy of the tube portion of the fluid-tube cantilever
t	time variable
U	dimensional space-average flow velocity in the tube
$u(x; t)$	dimensional axial displacement
$V_{\mathrm{F}}(t)$	potential energy of the fluid portion of the fluid-tube cantilever
$V_{\mathrm{T}}(t)$	potential energy of the tube portion of the fluid-tube cantilever
$\mathbf{v}_F(x; t)$	velocity vector of the fluid element
$\mathbf{v}_T(x; t)$	velocity vector of the tube element
$v(x; t)$	in-plane displacement along the y-axis
$w(x; t)$	out-of-plane displacement along the z-axis
x	coordinate position on the x-axis
α	nondimensional complex circular frequency of lateral vibrations
β	density ratio
δ	Kroneckers delta ; see equation (33)
ζ	nondimensional axial position variable
$\eta(\zeta; \tau)$	nondimensional displacement variable for out-of-plane lateral vibrations
η_0	nondimensional angular speed of rotation of the rotating fluid-tube cantilever beam
λ_r	the rth eigenvalue of the flexible cantilever beam
$\xi(\zeta; \tau)$	nondimensional displacement variable for in-plane lateral vibrations
ρ_F	fluid mass per unit volume
σ_r	nondimensional coefficient in the normalized eigenfunctions of the flexible cantilever beam H_r
τ	nondimensional time variable
υ	nondimensional speed of inner flow
υ_{cr}	critical nondimensional speed of inner flow
$\upsilon_{\mathrm{cr/in}}$	in-plane critical nondimensional speed of flow of the rotating fluid-tube cantilever system
$\upsilon_{\mathrm{cr/out}}$	out-of-plane critical nondimensional speed of flow of the rotating fluid-tube cantilever system
ϕ	nondimensional position variable
ψ	dimensional position variable
$\mathbf{\Omega}_0$	dimensional angular velocity vector of the rotating fluid-tube cantilever system
ω	nondimensional circular frequency of lateral vibration
ω_{cr}	critical nondimensional circular frequency of lateral vibration of the rotating fluid-tube cantilever system
$\omega_{\mathrm{cr/in}}$	value of ω_{cr} for in-plane lateral vibration of the rotating fluid-tube cantilever system
$\omega_{\mathrm{cr/out}}$	value of ω_{cr} for out-of-plane lateral vibration of the rotating fluid-tube cantilever system
$\omega_{\mathrm{cr/nf}}$	value of ω_{cr} for lateral vibration of the rotating cantilever system without fluid